Egypt. J. Chem. **Vol. 64,** No. 3 pp. 1149 - 1166 (2021)

Egyptian Journal of Chemistry

http://ejchem.journals.ekb.eg/

Molecular Modeling Analyses of Polyvinyl Alcohol/ Sodium Alginate/ZnO Composite

Ahmed Fahmy[a,*], Rasha M. Khafagy[b], Hanan Elhaes[b], Medhat A. Ibrahim[a]

[a] *Molecular Spectroscopy and Modeling Unit, Spectroscopy Department, National Research Centre, 33 El-Bohouth St., 12622 Dokki, Giza, Egypt*

[b] *Physics Department, Faculty of Women for Arts, Science, and Education, Ain Shams University, 11757 Cairo, Egypt*

Abstract

Molecular modeling analyses based on density functional theory (DFT) is considered as a promising tool for elucidating different properties of polymeric materials on the molecular scale. So that, the electronic properties of polyvinyl alcohol (PVA)/sodium alginate (Na Alg)/ zinc oxide (ZnO) are conducted with B3LYP/6-311g (d,p) level. Some physical parameters like total dipole moment (TDM), HOMO/LUMO band gap energy, molecular electrostatic potential (MESP), quantitative structure activity relationship (QSAR) and finally some thermal descriptors are calculated. The obtained results of TDM and HOMO/LUMO band gap energies dedicated that a considerable change occurred in the electronic structure of the studied models. Also, molecular electrostatic potential results confirmed the results of TDM and HOMO/LUMO energy gaps. Meanwhile, the calculated QSAR and thermal descriptors ensure the results obtained by DFT calculations whereas their values reflecting higher reactive structures. This verifies the impact of modifying the proposed polymer blend with nano ZnO according to its unique physical and electronic characteristics in nano scale.

Keywords: DFT; PVA; Na Alg; ZnO; QSAR; Thermal parameters..

1. Introduction:

Na Alg is a derivative of alginic acid belonging to polysaccharide family, some details about its molecular and chemical structure is described earlier [1-3]. It has the same features of biopolymers so that it is widely dedicated to many applications beside biocompatibility, biodegradability, it is water soluble and easy handled and could be functionalized [4-7]. The existence of reactive functional groups such as carboxyl group enhances reactivity, while further applications could be achieved after chemical modifications [8,9]. Although PVA is non-biodegradable sources, but has several advantages enable its applications in several fields [10-12]. Accordingly, it is widely used to enhance the properties of biopolymers when they blended together [13-15]. Non toxic and stable metal oxides such as ZnO still of extensive interest in many fields of applications [16, 17]. ZnO in nano scale show small size effect as well as larger specific surface area which dedicate it for many applications [18] especially as good antibacterial agent according to its inhibition ability [19, 20]. Bio-based nanocomposites including synthetic and biopolymers together with nano metal oxides are design to obtain so called extraordinary multifunctional properties serve in many area of research [21- 27].

On the other hand, alginate in the form membrane could be loaded with nano ZnO [28], the produce membrane show potential for biomedical as well as environmental applications. Alginate could be prepared in the form of gel then ZnO could be loaded. The resultant PVA/ZnO act as antibacterial agents and show effects on Bacillus cereus and Pseudomonas aerigunosa [29]. Cellulose which is another member of polysaccharides could be

*Corresponding author e-mail: ahmed_fahmy1994@yahoo.com.; (Ahmed Fahmy).
Receive Date: 30 December 2020, Accept Date: 15 January 2021
DOI: 10.21608/EJCHEM.2021.55865.3184

also loaded with nano ZnO. It is stated that the existence of Na Alg in this blend could enhances the mechanical properties [30]. The medical applications for polysaccharides including cellulose, chitosan, and alginate hydrogels loaded withnZnO are surveyed [31].

To investigate physical, chemical and biological properties of different macromolecules molecular modeling with different level of theories considered as the best choice for such investigations [32-37]. Molecular modeling at semi-empirical PM6 and DFT levels were utilized to investigate the electronic properties of PVA/Na Alg [38].

Based on this work further enhancement in the electronic properties of PVA/ Na Alg is achieved as ZnO is introduced. Accordingly, this work is conducted to calculate MESP, TDM and the difference between the highest and the lowest molecular orbital HOMO/LUMO band gap energy at B3LYP/6-311g (d,p) level then use QSAR to calculate some important descriptors

2. Calculation details:

Model molecules representing PVA, Na Alg, and PVA/ Na Alg /ZnO are subjected to calculations using Gaussian 09 software [39] at Spectroscopy Department, National Research Centre, Egypt. Also, physical parameters such as: TDM; HOMO/LUMO energy gap and MESP are calculated at DFT: B3LYP [40- 42] using the basis set 6-311g (d,p). Moreover, QSAR descriptors and some thermal parameters are computed using SCIGRESS packages at PM6 level at Spectroscopy Department, National Research Centre, Egypt.

3. Results and discussions

3.1 Building molecules

The proposed structures of PVA and Na Alg which introduced to study the effect of metal oxide addition are trimer PVA and dimer Na Alg. The interaction of PVA with Na Alg proceeds through the hydroxyl groups of PVA, as PVA in its trimer form consists of 3 groups. Previously, it is stated that the simulated model of 3PVA- (C_{10}) 2 Na Alg and that of Term 1 Na Alg - 3PVA- Mid 1 Na Alg are the most probable interactions to occur. This is because they have the highest TDM and lowest HOMO/LUMO energy gaps in comparison with the rest of the studied structures. The two structures: 3PVA- (C_{10}) 2 Na Alg and that of Term 1 Na Alg - 3PVA- Mid 1 Na Alg means that trimer PVA can interact with Na Alg in two different ways. The first is that the two units of Na Alg as a bulk can interact with 3PVA at any OH group position. Meanwhile, the second way is that each unit of 2 Na Alg can interact separately with 3PVA at different positions [38]. So that, the metal oxide is supposed to interact with trimer PVA and dimer Na Alg through the following two structures: 2 Na Alg 3PVA- (C_{10}) 2 Na Alg and that of Term 1 Na Alg - 3PVA- Mid 1 Na Alg. As the structures of the studied polymers are very rich with hydroxyl groups, therefore the interaction with the metal oxide processed only through the OH groups. The metal oxide studied here is ZnO. So that, as the structure of 3PVA- (C_{10}) 2 Na Alg contains five hydroxyl groups (OH) then different concentrations of ZnO can be added started from one unit up to five units. However, there are two possibilities for the interaction wither it proceeds through the Zn atom or O atom. Similarly for the structure of Term 1 Na Alg - 3PVA- Mid 1 Na Alg where, there are five OH groups available. The interaction between the studied structure of Term 1 Na Alg - 3PVA- Mid 1 Na Alg and1, 2, 3, 4 and 5 units of ZnO respectively is only weak interaction. However, there are two probabilities for the interaction of ZnO with the supposed structures. Where, the interaction may be done throughout the metal atom or the oxygen atom of the metal oxide. Therefore, in the present work the two probabilities are studied for the two structures of 3PVA- (C_{10}) 2 Na Alg and Term 1 Na Alg - 3PVA- Mid 1 Na Alg.

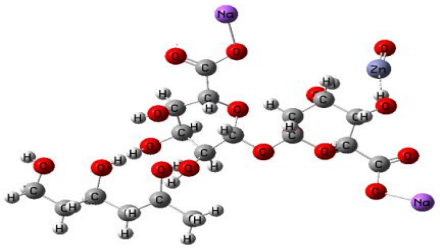

(a)

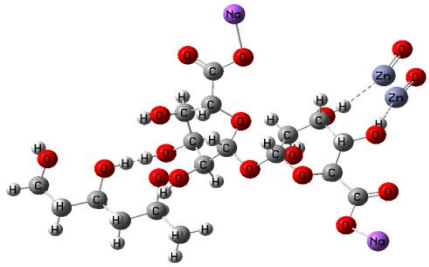

(b)

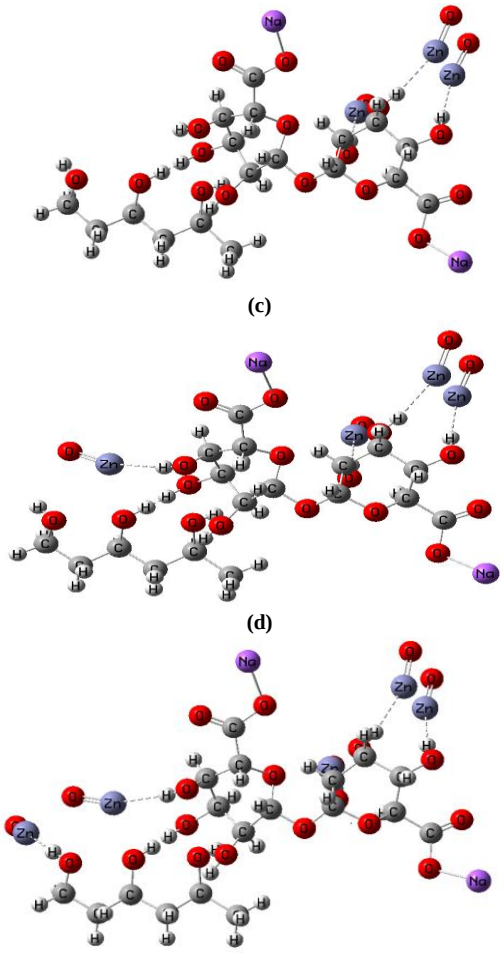

Fig. 1. B3LYP/6-311G(d,p) optimized structures of a- 3PVA- (C_{10}) 2 Na Alg - 1ZnO; b- 3PVA- (C_{10}) 2 Na Alg - 2ZnO; c- 3PVA- (C_{10}) 2 Na Alg - 3ZnO; d- 3PVA- (C_{10}) 2 Na Alg - 4ZnO and e- 3PVA- (C_{10}) 2 Na Alg - 5ZnO. The weak interaction proceeds through Zn atom

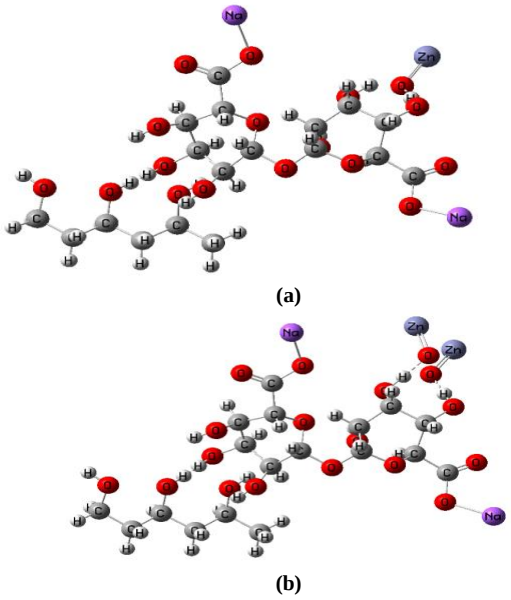

Fig. 2. B3LYP/6-311G(d,p) optimized structures of a- 3PVA- (C_{10}) 2 Na Alg - 1OZn; b- 3PVA- (C_{10}) 2 Na Alg - 2OZn; c- 3PVA- (C_{10}) 2 Na Alg - 3OZn; d- 3PVA- (C_{10}) 2 Na Alg - 4OZn and e- 3PVA- (C_{10}) 2 Na Alg - 5OZn. The weak interaction proceeds through oxygen atom

Figure 1 and figure 2 show the simulated structures of 3PVA- (C_{10}) 2 Na Alg interacted with 1, 2, 3, 4 and 5 units of metal oxide through the metal atom and through the oxygen atom respectively. However, figures 3 and 4 shows the structures representing Term 1 Na Alg - 3PVA- Mid 1 Na Alg interacted with 1, 2, 3, 4, 5 and 6 units of the metal oxide throughout the metal atom and the oxygen atom respectively.

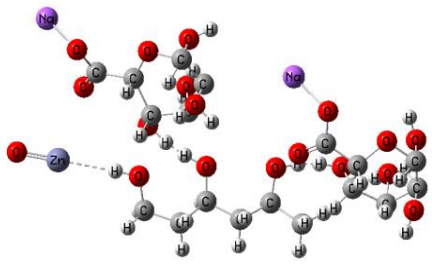

(a)

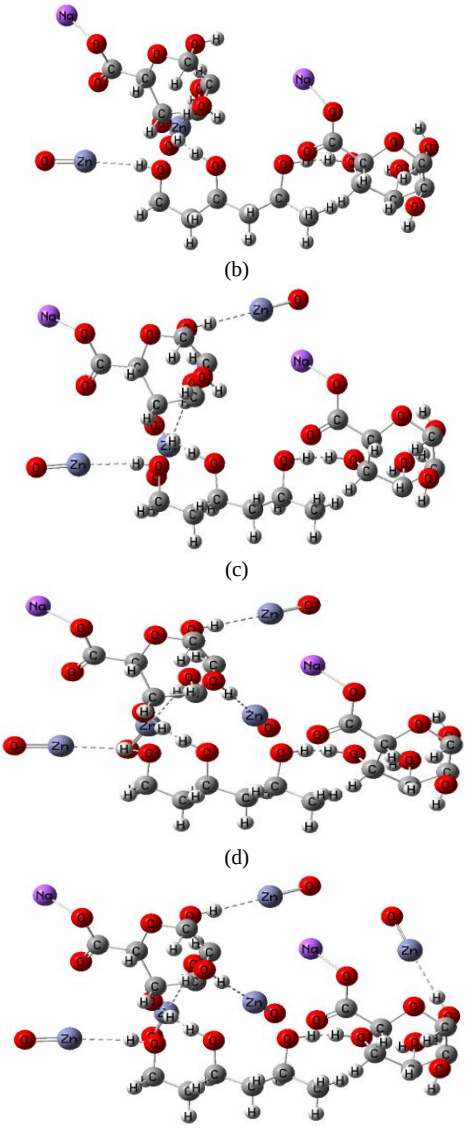

(b) (c) (d) (e)

Fig. 3. B3LYP/6-311G(d,p) optimized structures of a- Term 1 Na Alg - 3PVA- Mid 1 Na Alg - 1ZnO; b- Term 1 Na Alg - 3PVA- Mid 1 Na Alg - 2ZnO; c- Term 1 Na Alg - 3PVA- Mid 1 Na Alg - 3ZnO; d- Term 1 Na Alg - 3PVA- Mid 1 Na Alg - 4ZnO; and e- Term 1 Na Alg - 3PVA- Mid 1 Na Alg - 5ZnO. The weak interaction proceeds through Zn atom

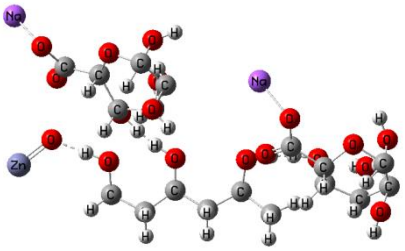

(a)

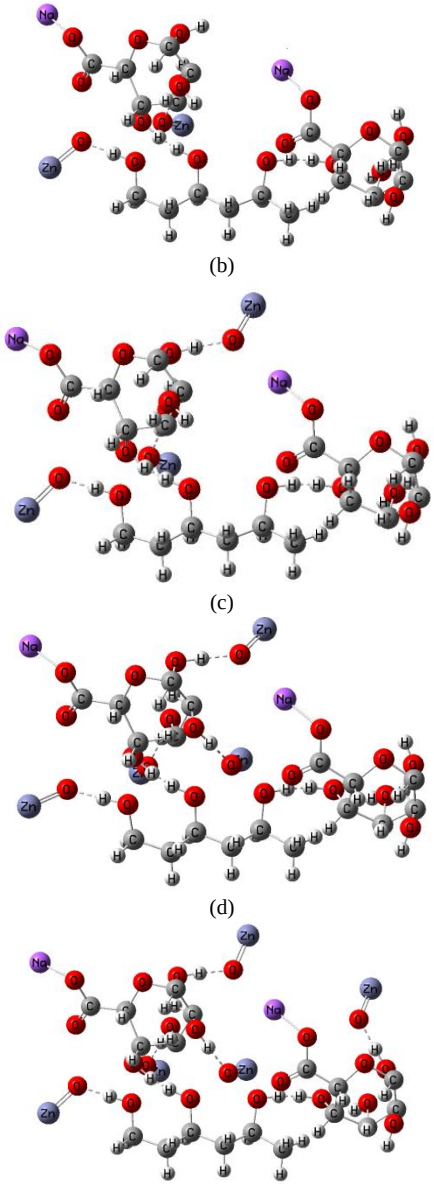

(b) (c) (d) (e)

Fig. 4. B3LYP/6-311G(d,p) optimized structures of a- Term 1 Na Alg - 3PVA- Mid 1 Na Alg - 1OZn; b- Term 1 Na Alg - 3PVA- Mid 1 Na Alg - 2OZn; c- Term 1 Na Alg - 3PVA- Mid 1 Na Alg - 3OZn; d- Term 1 Na Alg - 3PVA- Mid 1 Na Alg - 4OZn and e- Term 1 Na Alg - 3PVA- Mid 1 Na Alg - 5OZn. The weak interaction proceeds through oxygen atom

3.2 Total dipole moment and HOMO/LUMO energy gap calculation:

Based on the previous studies on the electronic properties of polymeric materials, it is noticed that the interpretation of TDM, HOMO/LUMO energies and MESP values becomes very important. So that, TDM, HOMO/LUMO energies and MESP are calculated for all interaction possibilities at the same level of DFT using the same bases set.

Table 1. B3LYP/6-311G (d,p) calculated total dipole moment (TDM) as Debye; HOMO/LUMO band gap energies (ΔE) as eV for 3PVA- C_{10} 2 Na Alg - X ZnO where X= 1, 2, 3, 4 and 5

Structure	TDM	ΔE
3PVA- C_{10} 2 Na Alg - 1ZnO	18.9005	0.2890
3PVA- C_{10} 2 Na Alg - 2ZnO	89.8929	0.2612
3PVA- C_{10} 2 Na Alg - 3ZnO	19.8118	0.3048
3PVA- C_{10} 2 Na Alg - 4ZnO	21.9045	0.3576
3PVA- C_{10} 2 Na Alg - 5ZnO	29.1104	0.3502

Table 2. B3LYP/6-311G (d,p) calculated total dipole moment (TDM) as Debye; HOMO/LUMO band gap energies (ΔE) as eV for 3PVA- C10 2 Na Alg - X OZn where X= 1, 2, 3, 4 and 5

Structure	TDM	ΔE
3PVA- C_{10} 2 Na Alg - 1OZn	11.4709	0.3380
3PVA- C_{10} 2 Na Alg - 2OZn	14.4875	0.3034
3PVA- C_{10} 2 Na Alg - 3OZn	14.0818	0.3682
3PVA- C_{10} 2 Na Alg - 4OZn	5.3791	0.3306
3PVA- C_{10} 2 Na Alg - 5OZn	10.1023	0.2863

Table 3. B3LYP/6-311G (d,p) calculated total dipole moment (TDM) as Debye; HOMO/LUMO band gap energies (ΔE) as eV for Term 1 Na Alg-3PVA-Mid 1 Na Alg-X ZnO where X= 1, 2, 3, 4 and 5

Structure	TDM	ΔE
Term 1 Na Alg-3PVA-Mid 1 Na Alg - 1ZnO	13.0203	1.4724
Term 1 Na Alg-3PVA-Mid 1 Na Alg - 2ZnO	13.4947	0.8754
Term 1 Na Alg -3PVA-Mid 1 Na Alg-3ZnO	8.7693	0.3495
Term 1 Na Alg-3PVA-Mid 1 Na Alg - 4ZnO	8.8606	0.5521
Term 1 Na Alg-3PVA-Mid 1 Na Alg - 5ZnO	11.5282	0.5551

Table 4. B3LYP/6-311G (d,p) calculated total dipole moment (TDM) as Debye; HOMO/LUMO band gap energies (ΔE) as eV for Term 1 Na Alg-3PVA-Mid 1 Na Alg-X OZn where X= 1, 2, 3, 4 and 5

Structure	TDM	ΔE
Term 1 Na Alg-3PVA-Mid 1 Na Alg-1OZn	20.4159	0.2201
Term 1 Na Alg-3PVA-Mid 1 Na Alg-2OZn	21.7218	0.2294
Term 1 Na Alg-3PVA-Mid 1 Na Alg - 3OZn	22.1593	0.2308
Term 1 Na Alg-3PVA-Mid 1 Na Alg - 4OZn	20.6782	0.4713
Term 1 Na Alg-3PVA-Mid 1 Na Alg - 5OZn	20.0846	0.4683

Table 5. PM6 calculated QSAR parameters including final heat of formation (HF) as kcal/mol, total dipole moment (TDM) as Debye, HOMO/LUMO band gap energy (ΔE) as eV and ionization potential (IP) as eV

Structure		FF (kcal/mol)	TDM (Debye)	Δ***E*** (eV)	IP (eV)
3PVA- C10 2 Na Alg		-858.075	5.261	9.554	-9.744
3PVA- C_{10}2 Na Alg	1ZnO	-900.085	6.762	9.892	-9.859
	2ZnO	-1187.763	10.846	8.376	-10.102
	3ZnO	-4477.774	15.038	7.209	-8.662
	4ZnO	-4413.364	7.762	7.626	-9.413
	5ZnO	-4661.310	5.761	7.375	-9.717
	1OZn	-838.259	14.916	7.453	-9.136
	2 OZn	-910.966	8.232	5.677	-8.199
	3 OZn	-1260.523	20.546	6.268	-8.899
	4 OZn	-1278.845	12.883	4.721	-9.722
	5 OZn	-1458.557	12.345	4.372	-9.368
Term 1 Na Alg - 3PVA - Mid 1 Na Alg		-885.059	14.910	7.883	-9.385
Term 1 Na Alg -3PVA - Mid 1 Na Alg	1 ZnO	-1762.517	26.162	5.595	-9.047
	2 ZnO	-1705.777	6.819	6.364	-9.548
	3 ZnO	-1990.253	1.708	6.975	-9.766
	4 ZnO	-1705.777	6.819	6.364	-9.548
	5 ZnO	-1004.023	3.120	7.564	-8.956
	1 OZn	-1152.312	3.962	6.596	-7.599
	2 OZn	-1590.752	5.935	7.571	-8.761
	3 OZn	-1824.065	15.691	7.13	-10.619
	4 OZn	-1873.991	13.051	4.453	-8.820
	5 OZn	-1130.011	3.258	9.552	-9.823

Table 1 and table 3 present the changes occurred in the TDM and HOMO/LUMO energy for the proposed structures of 3PVA- (C_{10}) 2 Na Alg and Term 1 Na Alg - 3PVA- Mid 1 Na Alg as a result of the interaction with the ZnO throughout the zinc atom. As presented in ref. [38], the simulated models of 3PVA- (C_{10}) 2 Na Alg and Term 1 Na Alg - 3PVA- Mid 1 Na Alg possesses TDM of 12.2080 and 24.6199 Debye and HOMO/LUMO band gap energies of 0.2908 and 0.5706 eV respectively. It is clear from table 1 that the TDM value of 3PVA- (C_{10}) 2 Na Alg was changed greatly due to the interaction with ZnO throughout the zinc atom. Where, it increased to 18.9005, 89.8929, 19.8118, 21.9045 and 29.1104 Debye for the interaction with 1, 2, 3, 4 and 5 units of ZnO as presented in table 2. However, the HOMO/LUMO band gaps become 0.2890, 0.2612, 0.3048, 0.3576 and 0.3502 eV respectively for 3PVA- (C_{10}) 2 Na Alg interacted with 1, 2, 3, 4 and 5 ZnO. The variation in the HOMO/LUMO energies for 3PVA- (C_{10}) 2 Na Alg interacted with ZnO throughout the Zn atom is presented in figure 5. On the other hand, for the interaction of 3PVA- (C_{10}) 2 Na Alg with the metal oxide through the oxygen atom, table 2 shows that the TDM was changed to 11.4709, 14.4875, 14.0818, 5.3791 and 10.1023 Debye. Meanwhile, HOMO/LUMO energy gap changed to 0.3380, 0.3034, 0.3682, 0.3306 and 0.2863eV for the interaction of 3PVA- (C_{10}) 2 Na Alg with 1, 2, 3, 4 and 5 units of OZn respectively as shown in figure 6.

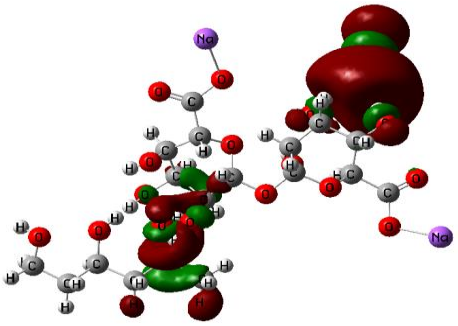

(a)

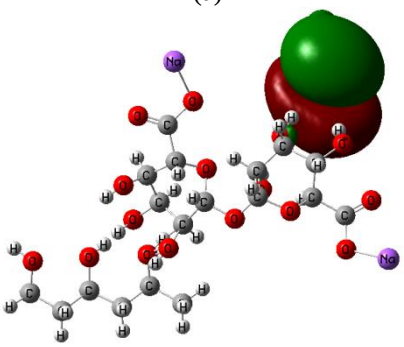

(b)

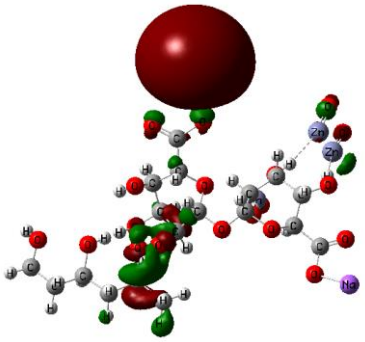

(c)

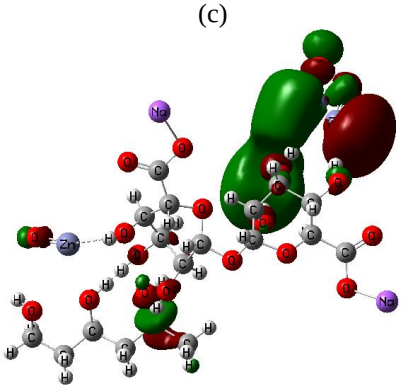

(d)

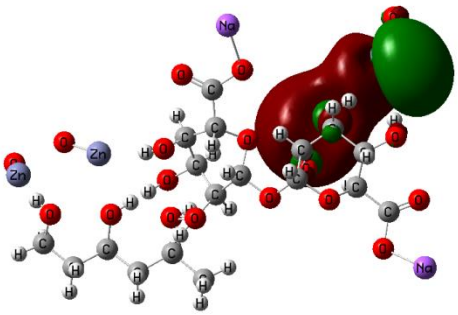

(e)

Fig. 5. B3LYP/6-311G(d,p) calculated HOMO/LUMO band gap energy of a- 3PVA- (C_{10}) 2 Na Alg - 1ZnO; b- 3PVA- (C_{10}) 2 Na Alg - 2ZnO; c- 3PVA- (C_{10}) 2 Na Alg - 3ZnO; d- 3PVA- (C_{10}) 2 Na Alg - 4ZnO and e- 3PVA- (C_{10}) 2 Na Alg - 5ZnO. The weak interaction proceeds through Zn atom

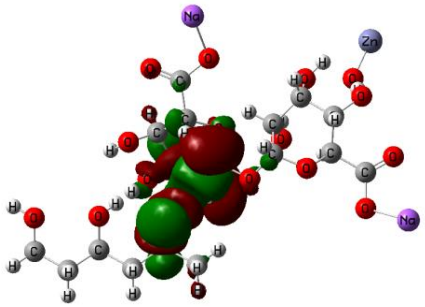

(a)

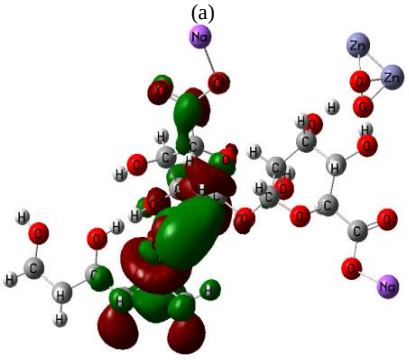

(b)

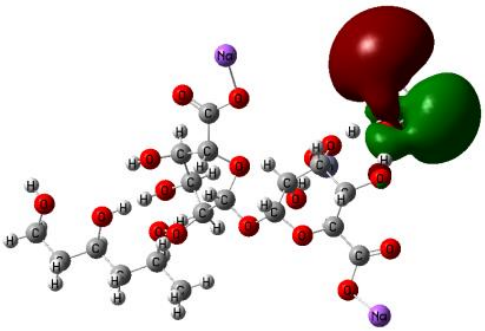

(c)

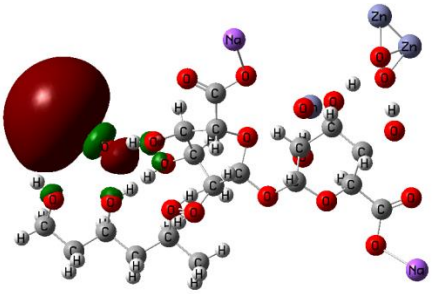

(d)

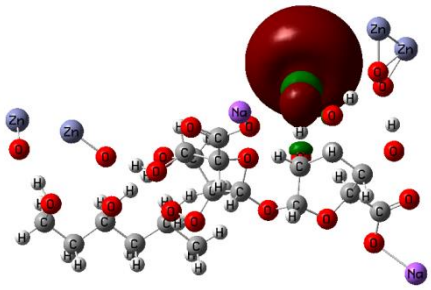

(e)

Fig. 6. B3LYP/6-311G(d,p) calculated HOMO/LUMO band gap energy of a- 3PVA- (C_{10}) 2 Na Alg - 1OZn; b- 3PVA- (C_{10}) 2 Na Alg - 2OZn; c- 3PVA- (C_{10}) 2 Na Alg - 3OZn; d- 3PVA- (C_{10}) 2 Na Alg - 4OZn and e- 3PVA- (C_{10}) 2 Na Alg - 5OZn. The weak interaction proceeds through oxygen atom

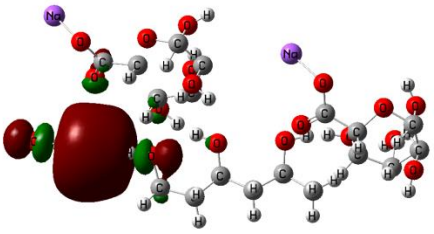

(a)

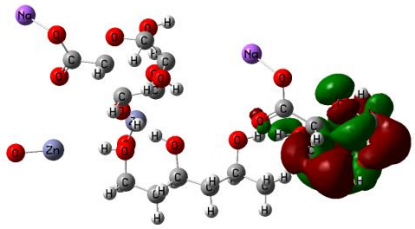

(b)

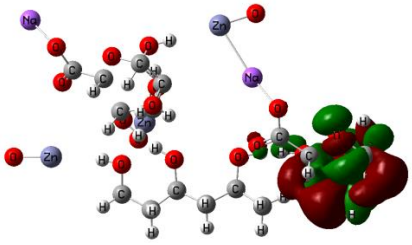

(c)

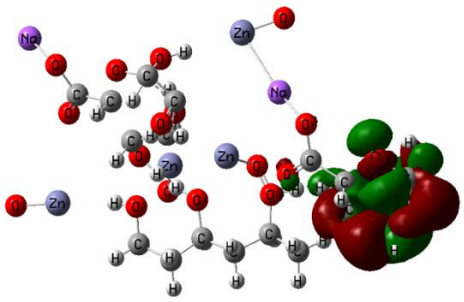

(d)

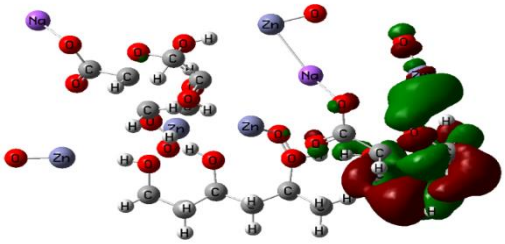

(e)

Fig. 7. B3LYP/6-311G(d,p) calculated HOMO/LUMO band gap energy of a- Term 1 Na Alg - 3PVA- Mid 1 Na Alg - 1ZnO; b- Term 1 Na Alg - 3PVA- Mid 1 Na Alg - 2ZnO; c- Term 1 Na Alg - 3PVA- Mid 1 Na Alg - 3ZnO; d- Term 1 Na Alg - 3PVA- Mid 1 Na Alg - 4ZnO and e- Term 1 Na Alg - 3PVA- Mid 1 Na Alg - 5ZnO. The weak interaction proceeds through Zn atom

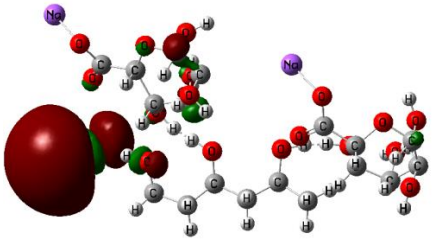

(a)

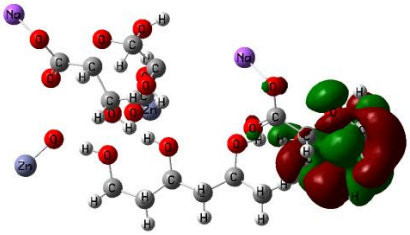

(b)

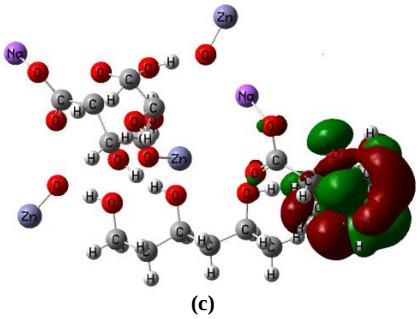

(c)

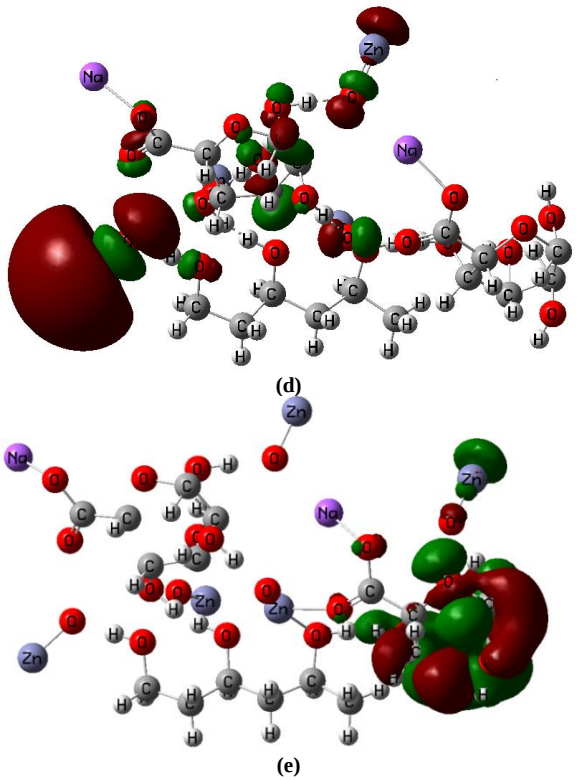

Fig. 8. B3LYP/6-311G(d,p) calculated HOMO/LUMO band gap energy of a- Term 1 Na Alg - 3PVA- Mid 1 Na Alg - 1OZn; b- Term 1 Na Alg - 3PVA- Mid 1 Na Alg - 2OZn; c- Term 1 Na Alg - 3PVA- Mid 1 Na Alg - 3OZn; d- Term 1 Na Alg - 3PVA- Mid 1 Na Alg - 4OZn and e- Term 1 Na Alg-3PVA-Mid 1 Na Alg - 5OZn. The weak interaction proceeds through oxygen atom

On contrast for the second structure (i.e. Term 1 Na Alg - 3PVA- Mid 1 Na Alg), TDM was influenced greatly and decreased to 13.0203, 13.4947, 8.7693, 8.8606 and 11.5282 Debye for Term 1 Na Alg - 3PVA- Mid 1 Na Alg - 1ZnO, Term 1 Na Alg - 3PVA- Mid 1 Na Alg - 2ZnO, Term 1 Na Alg - 3PVA- Mid 1 Na Alg - 3ZnO, Term 1 Na Alg - 3PVA- Mid 1 Na Alg - 4ZnO and Term 1 Na Alg - 3PVA- Mid 1 Na Alg - 5ZnO respectively. Meanwhile, HOMO/LUMO energy gap changed to 1.4724, 0.8754, 0.3495, 0.5521 and 0.5551 eV for the same sequence as presented in table 3. The changes occurred in the HOMO/LUMO energy gaps for these structures are presented in figure 7.

Finally, for the interaction of Term 1 Na Alg - 3PVA- Mid 1 Na Alg and the metal oxide that proceeds throughout the oxygen atom, both quantities are changed considerably. Where, as tabulated in table 4, TDM decreased slightly and becomes 20.4159,21.7218, 22.1593, 20.6782 and 20.0846 Debye for Term 1 Na Alg - 3PVA- Mid 1 Na Alg - 1OZn, Term 1 Na Alg - 3PVA- Mid 1 Na Alg - 2OZn, Term 1 Na Alg - 3PVA- Mid 1 Na Alg - 3OZn, Term 1 Na Alg - 3PVA- Mid 1 Na Alg - 4OZn and Term 1 Na Alg - 3PVA- Mid 1 Na Alg - 5OZn respectively. But, the HOMO/LUMO energy becomes 0.2201, 0.2294, 0.2308, 0.4713 and 0.4683 eV, see figure 8, for Term 1 Na Alg - 3PVA- Mid 1 Na Alg - 1OZn, Term 1 Na Alg - 3PVA- Mid 1 Na Alg 2OZn, Term 1 Na Alg - 3PVA- Mid 1 Na Alg - 3OZn, Term 1 Na Alg - 3PVA- Mid 1 Na Alg - 4OZn and Term 1 Na Alg - 3PVA- Mid 1 Na Alg - 5OZn respectively.

3.3 Molecular electrostatic potential (MESP):

MESP of the studied models can be recognized as a distribution of the electronic charges within the structures under study. MESP is a significant physical property for understanding the active sites position whether it nucleophilic or electrophilic. Generally, MESP could be considered as a good descriptor for formation of hydrogen bonding between the studied models. In the present study, MESP is mapped as contours of all studied models. Figures 9, 10,11 and 12 present the calculated MESP at B3LYP/6-311G(d,p) level of DFT for: 3PVA-(C_{10}) 2 Na Alg - X ZnO, 3PVA- (C_{10}) 2 Na Alg -X OZn, Term 1 Na Alg - 3PVA- Mid 1 Na Alg - Y ZnO and Term 1 Na Alg - 3PVA- Mid 1 Na Alg - Y OZn where X and Y= 1, 2, 3, 4 and 5 respectively. To understand the contours of the mapped MESP, the MESP values at the surface are represented by colors ranging from red, orange, yellow, green to blue. Where the red color refers to the highest electrostatic energy and blue refers to the lowest electrostatic energy. The electrostatic potential energy decreases on going from red to the rest of the mentioned colors. The figures indicated that the red regions are localized only on the oxygen atoms. Where, as presented in figures 10 and 12 it is indicated that the intensity of the red color increased due to the decoration with ZnO throughout the O atom. This refers to the possible positions for electrophilic interaction. However, the figures indicated that the positive regions are centered at the Zn atom which refers to the possible positions for nucleophilic interaction. The obtained results of MESP are compatible with that of TDM and HOMO/LUMO energy.

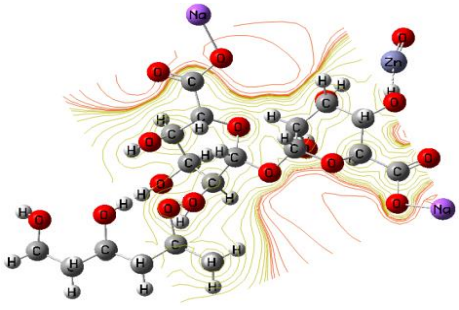

(a)

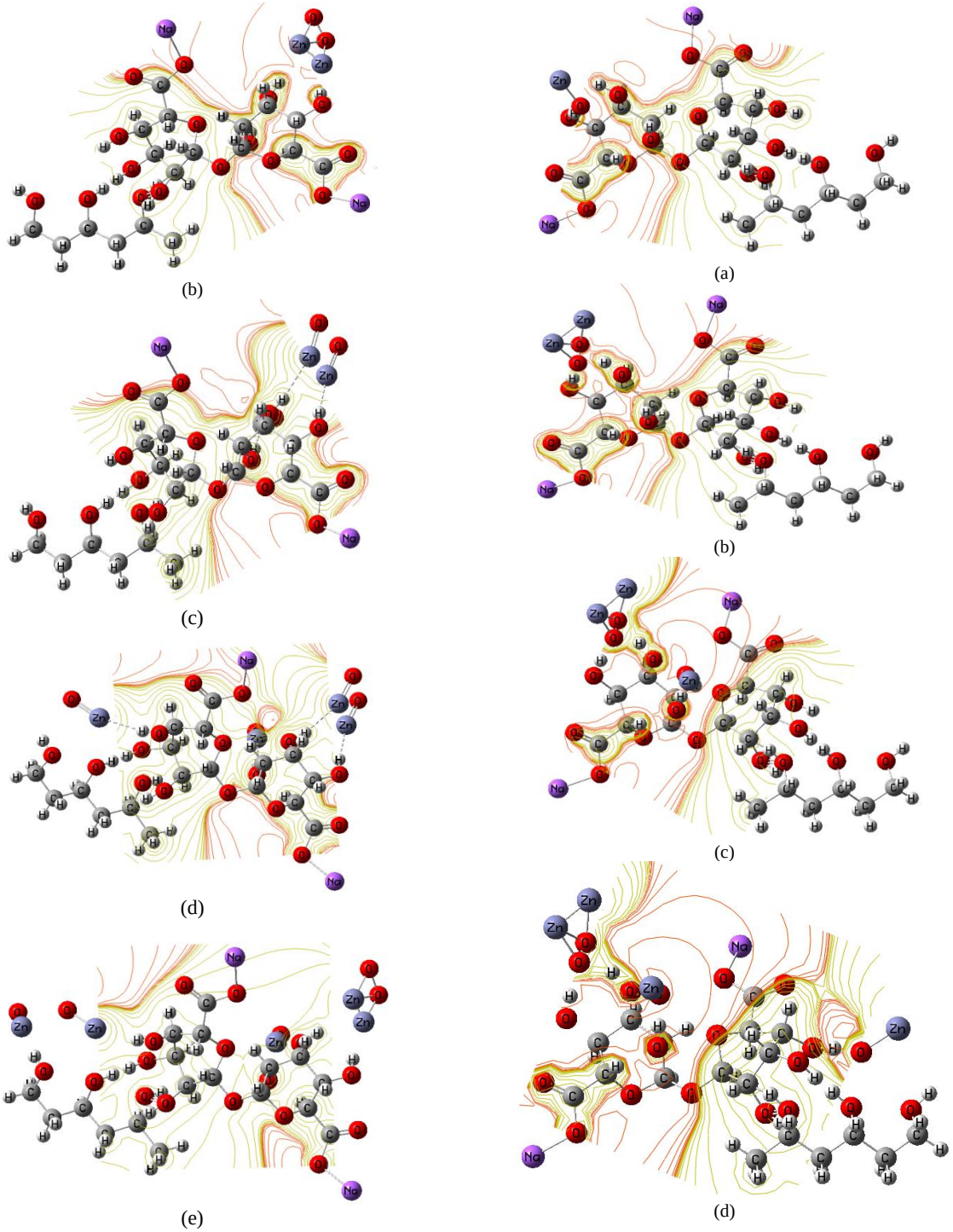

Fig. 9. B3LYP/6-311G(d,p) calculated MESP as contour of a- 3PVA- (C_{10}) 2 Na Alg - 1ZnO; b- 3PVA- (C_{10}) 2 Na Alg - 2ZnO; c- 3PVA- (C_{10}) 2 Na Alg - 3ZnO; d- 3PVA- (C_{10}) 2 Na Alg - 4ZnO and e- 3PVA- (C_{10}) 2 Na Alg - 5ZnO. The weak interaction proceeds through Zn atom

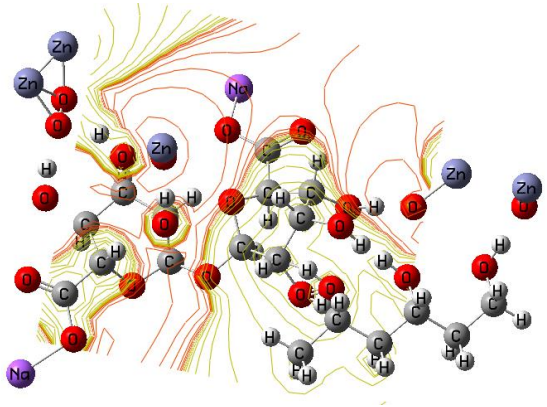

(e)

Fig. 10. B3LYP/6-311G(d,p) calculated MESP as contour of a- 3PVA- (C_{10}) 2 Na Alg-1 OZn; b- 3PVA- (C_{10}) 2 Na Alg - 2OZn; c- 3PVA- (C_{10}) 2 Na Alg - 3OZn; d- 3PVA- (C_{10}) 2 Na Alg - 4OZn and e- 3PVA- (C_{10}) 2 Na Alg - 5OZn. The weak interaction proceeds through oxygen atom

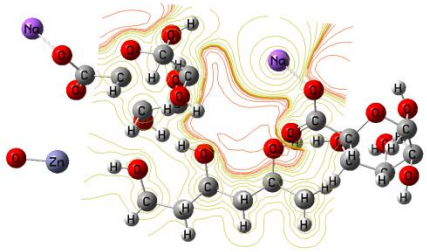

(a)

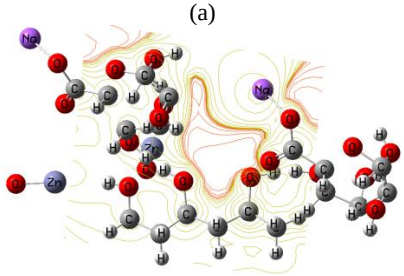

(b)

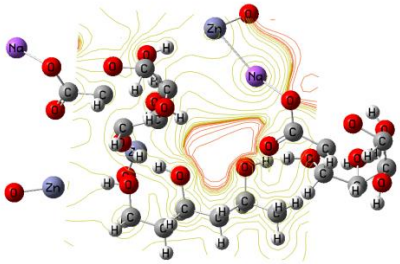

(c)

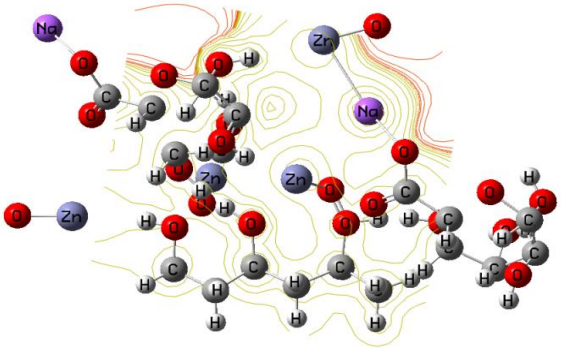

(d)

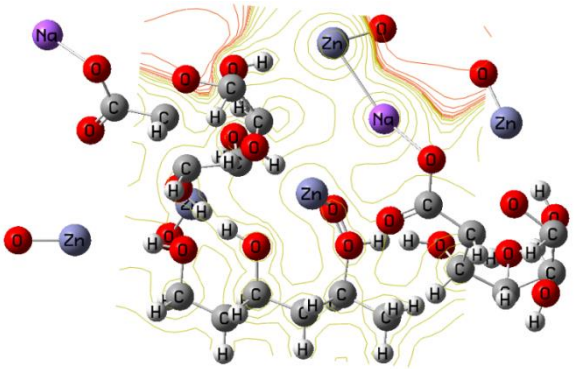

(e)

Fig. 11. B3LYP/6-311G(d,p) calculated MESP as contour of a- Term 1 Na Alg - 3PVA- Mid 1 Na Alg - 1ZnO; b- Term 1 Na Alg - 3PVA- Mid 1 Na Alg - 2ZnO; c- Term 1 Na Alg - 3PVA- Mid 1 Na Alg - 3ZnO; d- Term 1 Na Alg - 3PVA- Mid 1 Na Alg - 4ZnO and e- Term 1 Na Alg - 3PVA- Mid 1 Na Alg - 5ZnO. The weak interaction proceeds through Zn atom

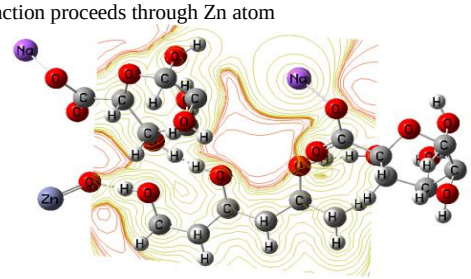

(a)

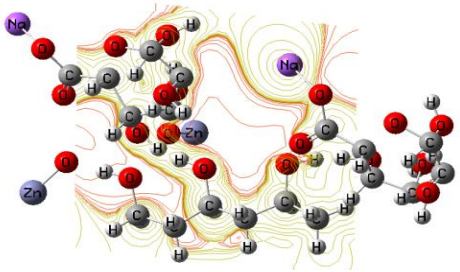

(b)

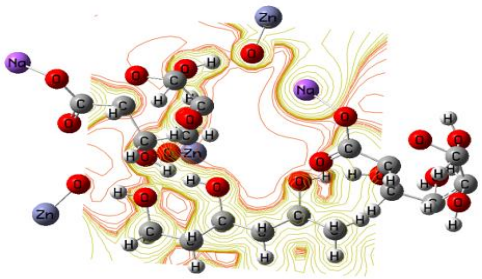

(c)

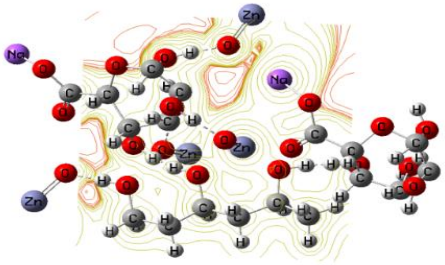

(d)

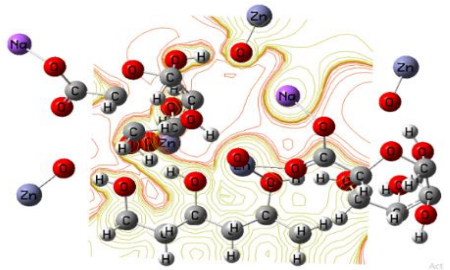

(e)

Fig. 12. B3LYP/6-311G(d,p) calculated MESP as contour of a- Term 1 Na Alg - 3PVA- Mid 1 Na Alg - 1OZn; b- Term 1 Na Alg - 3PVA- Mid 1 Na Alg - 2OZn; c- Term 1 Na Alg - 3PVA- Mid 1 Na Alg - 3OZn; d- Term 1 Na Alg - 3PVA- Mid 1 Na Alg - 4OZn and e- Term 1 Na Alg - 3PVA- Mid 1 Na Alg - 5OZn. The weak interaction proceeds through oxygen atom

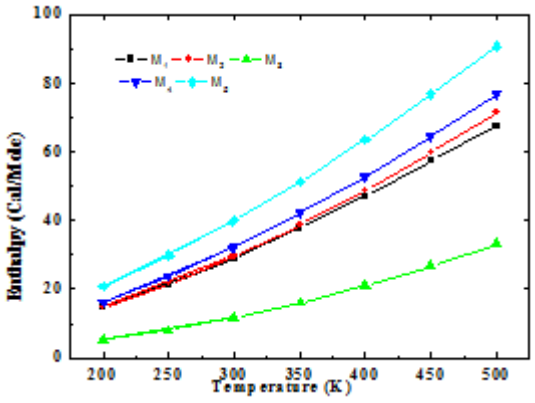

(a)

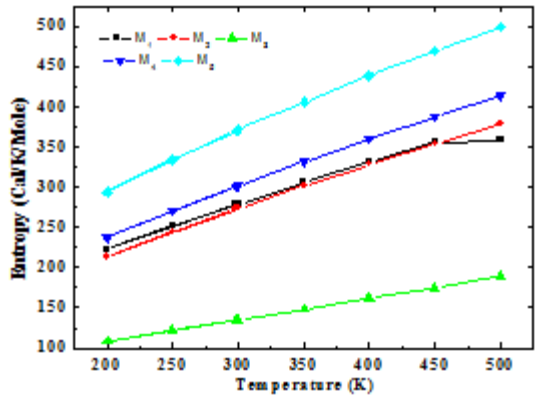

(b)

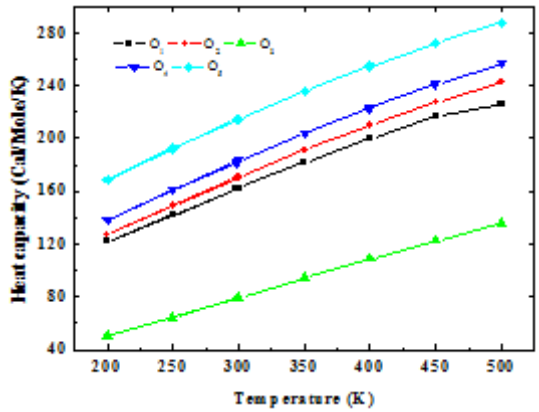

(c)

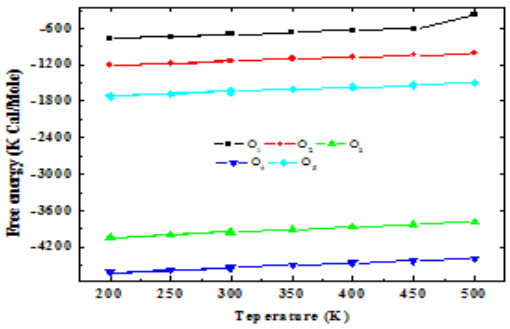

(d)

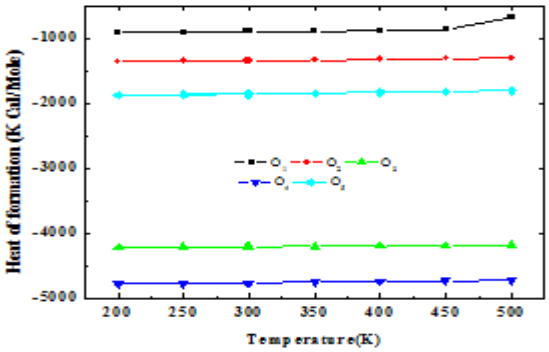

(e)

Fig. 13. PM6 calculated a) enthalpy , b) entropy , c) heat capacity , d) free energy and e) heat of formation for 3PVA – C_{10} 2 Na Alg - 1ZnO (i.e. sample M_1), 3PVA – C_{10} 2 Na Alg -2ZnO (i.e. sample M_2), 3PVA – C_{10} 2 Na Alg - 3ZnO (i.e. sample M_3) , 3PVA – C_{10} 2 Na Alg -4ZnO (i.e. sample M_4) and 3PVA – C_{10} 2 Na Alg -5ZnO (i.e. sample M_5) respectively

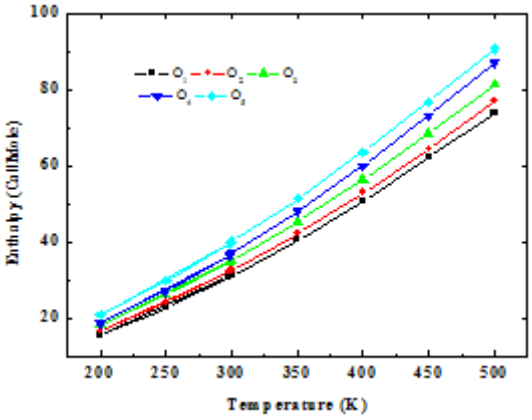

(a)

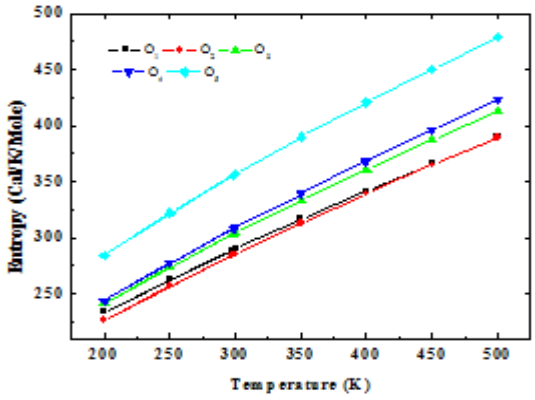

(b)

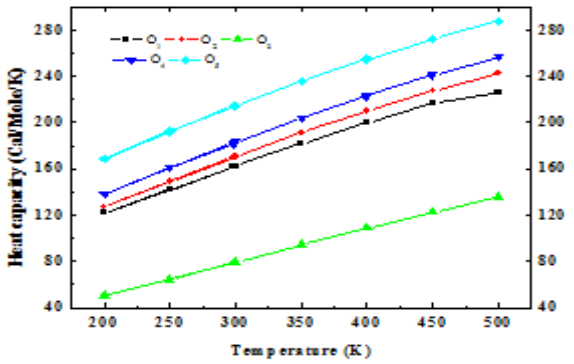

(c)

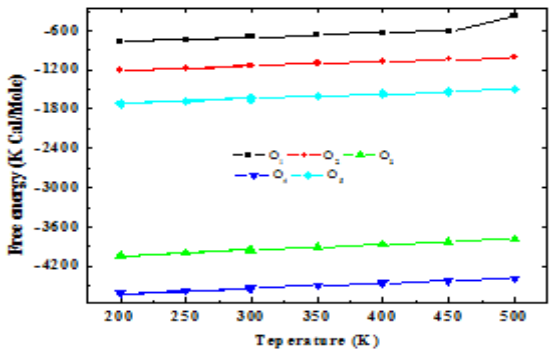

(d)

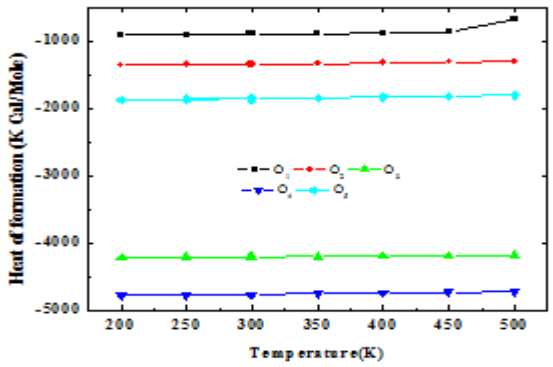

(e)

Fig. 14. PM6 calculated a) enthalpy, b) entropy , c) heat capacity , d) free energy and e) heat of formation for: 3PVA – C_{10} 2 Na Alg - 1OZn (i.e. sample O_1), 3PVA – C_{10} 2 Na Alg -2OZn (i.e. sample O_2), 3PVA – C_{10} 2 Na Alg - 3OZn (i.e. sample O_3), 3PVA – C_{10} 2 Na Alg -4OZn (i.e. sample O_4) and 3PVA – C_{10} 2 Na Alg -5OZn (i.e. sample O5) respectively

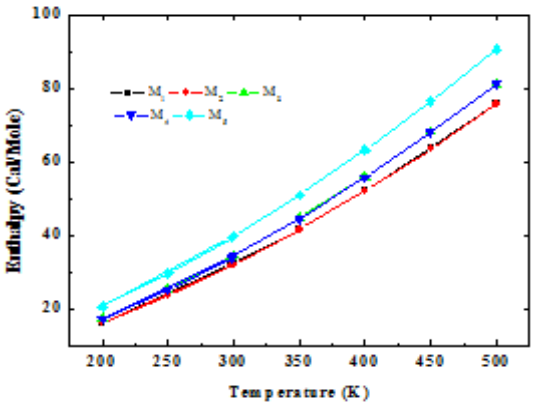

(a)

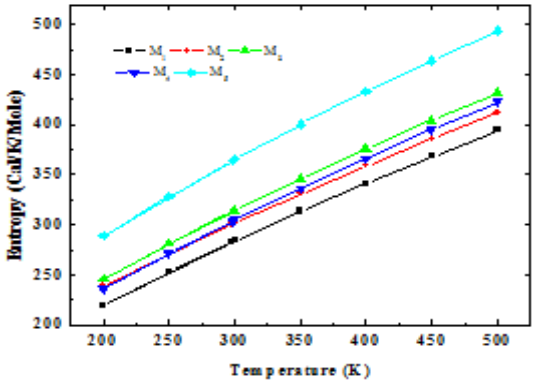

(b)

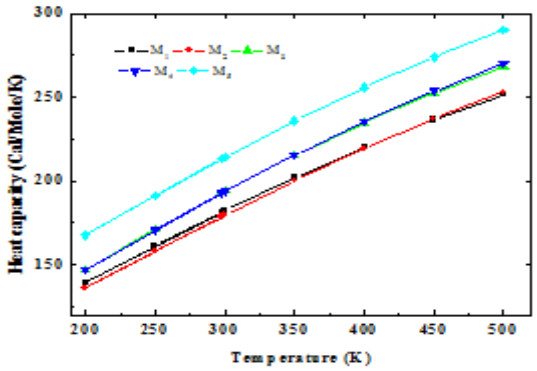

(c)

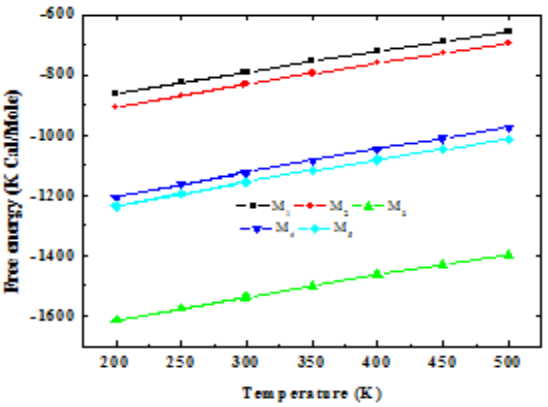

(d)

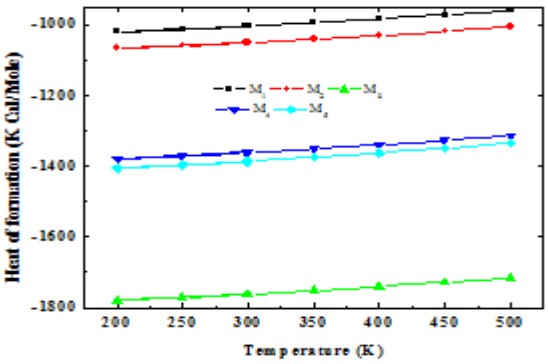

(e)

Fig. 15. PM6 calculated a) enthalpy , b) entropy , c) heat capacity , d) free energy and e) heat of formation for Term 1 Na Alg - 3PVA- Mid 1 Na Alg - 1ZnO (i.e. sample M_1), Term 1 Na Alg -

3PVA- Mid 1 Na Alg - 1ZnO (i.e. sample M_2), Term 1 Na Alg - 3PVA- Mid 1 Na Alg - 1ZnO (i.e. sample M_3), Term 1 Na Alg - 3PVA- Mid 1 Na Alg - 1ZnO (i.e. sample M_4) and Term 1 Na Alg - 3PVA- Mid 1 Na Alg - 1ZnO (i.e. sample M_5) respectively.

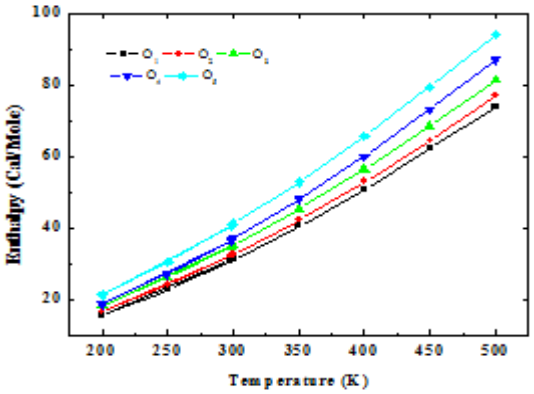

(a)

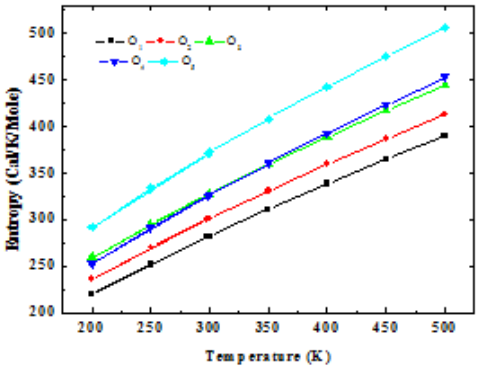

(b)

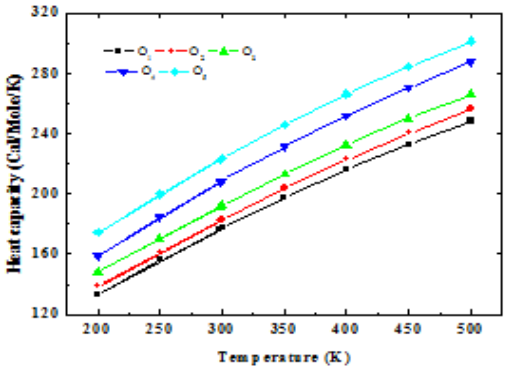

(c)

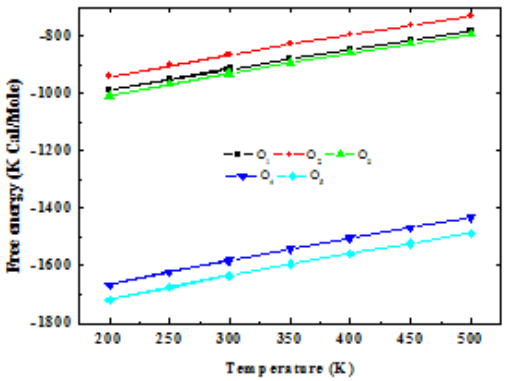

(d)

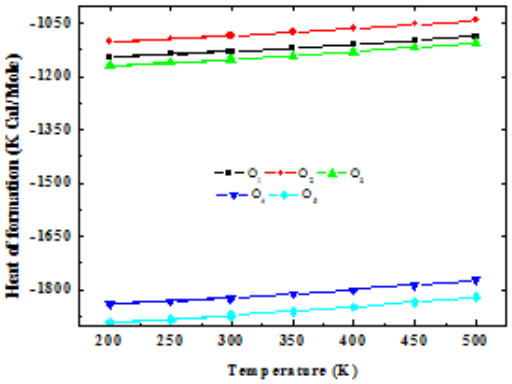

(e)

Fig. 16. PM6 calculated a) enthalpy , b) entropy , c) heat capacity , d) free energy and e) heat of formation for Term 1 Na Alg-3PVA-Mid 1 Na Alg-1OZn (i.e. sample O_1), Term 1 Na Alg-3PVA-Mid 1 Na Alg-2OZn (i.e. sample O_2), Term 1 Na Alg-3PVA-Mid 1 Na Alg-3OZn(i.e. sample O_3), Term 1 Na Alg-3PVA-Mid 1 Na Alg-4OZn (i.e. sample O_4) and Term 1 Na Alg - 3PVA- Mid 1 Na Alg - 5OZn (i.e. sample O_5)

3.4 QSAR Descriptors:

QSAR descriptors are calculated for the build structures at PM6 theoretical level. Table 5 lists the computed QSAR parameters such as final heat of formation (HF), TDM, HOMO/LUMO band gap energy (ΔE) and ionization potential (IP). Concerning FF that is termed as the change in heat accompanying the formation of some structure from its components. For the first group and second group named 3PVA-(C_{10}) 2 Na Alg -XZnO and 3PVA- (C_{10}) 2 Na Alg - XOZn , they have the same manner where their HF decreases as the number of ZnO species are increased from one to five through either Zn metal atom or O one. However, for 3PVA- (C_{10}) 2 Na Alg -XZnO, the largest HF value is -900 kcal for 3PVA- (C_{10}) 2 Na Alg -1ZnO while the lowest one is -4661.31 kcal for 3PVA- (C_{10}) 2 Na Alg -5ZnO. Meanwhile, for 3PVA- (C_{10}) 2 Na Alg -XOZn the largest one is -838.259 kcal for 3PVA- (C_{10}) 2 Na Alg -1OZn and the smallest one is -1458.557 kcal for 3PVA- (C_{10}) 2 Na Alg -5OZn. It is noticeable also that the HF results of those linked through Zn metal atom is much lower than those bonded through O one reflecting much higher thermal stability for them. On contrary, there is a fluctuation in the data of Term 1 Na Alg - 3PVA- Mid 1 Na Alg - (1ZnO:5ZnO) structures. The largest value is -1004.023 kcal for 3PVA Term-mid NaAlg-5ZnO and the smallest one is -1990.253 kcal for 3PVA Term-mid NaAlg-3ZnO. While Term 1 Na Alg - 3PVA- Mid 1 Na Alg - (1OZn:4OZn) have the same behavior of the first group where it decreases as the number of OZn species are increased from one to four units and reach to -1278.845 kcal. This is different for 5 OZn molecules where its FF is -1130.011 kcal. The largest value is -1152.312 kcal for Term 1 Na Alg - 3PVA-Mid 1 Na Alg -1OZn and the smallest one is -1873.991 kcal for Term 1 Na Alg - 3PVA- Mid 1 Na

Alg -4OZn. TDM as well as HOMO/LUMO band gap energy (ΔE) are strong physical indicators for structure reactivity. The higher the TDM, the higher the reactivity while the smaller the band gap, the higher the reactivity. Moreover, both TDM and HOMO/LUMO band gap energy are calculated again using semi-empirical method at PM6 level. For TDM of the first group named 3PVA- (C_{10}) 2 Na Alg, their TDM values increase as the number of ZnO metal oxide species are increased from one to three through Zn metal atom while addition of more fourth or fifth ZnO molecules cause fluctuation in their TDM values see table 5. Where, TDM values are 6.762, 10.846, 15.038, 7.762 and 5.761 Debye for 3PVA- (C_{10}) 2 Na Alg - (1ZnO:5ZnO). However, TDM of 3PVA- (C_{10}) 2 Na Alg -5OZnis the highest result among the second group. Where, the TDM values changed to 14.916, 8.232, 20.546, 12.883 and 12.345Debye ongoing from 1OZn to 5OZn together with 3PVA- (C_{10}) 2 Na Alg. For the third group, TDM of sample named Term 1 Na Alg - 3PVA- Mid 1 Na Alg -1ZnO has the highest TDM among this third group with values 26.162 Debye, indicating very reactive structure. However, TDM of Term 1 Na Alg - 3PVA- Mid 1 Na Alg -3ZnO is the smallest among all the proposed structures reflecting little reactivity level. Where, as presented in table 5, TDM equals 26.162, 6.819, 1.708, 6.819 and 3.120 Debye for Term 1 Na Alg - 3PVA- Mid 1 Na Alg -(1OZn:5OZn). In the fourth group, both Term 1 Na Alg - 3PVA- Mid 1 Na Alg -1OZn and Term 1 Na Alg - 3PVA- Mid 1 Na Alg -5OZn have nearly the same TDM and hence similar reactivity. This behavior is presented in table 5. Where, TDM for the fourth group changed to 3.962, 5.935, 15.691, 13.051 and 3.258 for Term 1 Na Alg - 3PVA- Mid 1 Na Alg -(1OZn:5OZn) respectively. ΔE results, calculated again at PM6 level of semi-empirical method, follow the same behavior of TDM ones. For the first group, ΔE decreases as ZnO number increase till reaches 7.375eV for 3PVA- (C_{10}) 2 Na Alg -5ZnO. Addition of OZn for the second group through the O atom has no impact on the band gap values. These results are clear in table 5, where ΔE becomes 9.892, 8.376, 7.209, 7.626 and 7.375 eV for 3PVA- (C_{10}) 2 Na Alg -(1ZnO:5 ZnO) and 7.453, 5.677, 6.268, 4.721, 4.372 eV for 3PVA- (C_{10}) 2 Na Alg -(1OZn:5 OZn) respectively instead of 9.554 eV. However, additions of ZnO through Zn or O atoms decrease reactivity except for Term 1 Na Alg - 3PVA- Mid 1 Na Alg - 4OZn. Finally, for IP, this is one of the QSAR parameters that reflect also structure reactivity. It is usually defined as the required energy for ionizing a chemical compound. IP of 3PVA- (C_{10}) 2 Na Alg - 2ZnO has the lowest IP values and hence the highest reactivity. However, the other proposed structures of the first group have a higher IP value that is about -9 eV. On the same manner, addition of ZnO for the third group till four ZnO molecules has no great effect on the results of IP, however it increases for those have five structures. Where, the IP values are -9.047, -9.548, -9.766, -9.548 and -8.956 eV for Term 1 Na Alg - 3PVA- Mid 1 Na Alg -(1ZnO:5ZnO) respectively instead of -9.385eV for Term 1 Na Alg - 3PVA- Mid 1 Na Alg. Addition of ZnO for the fourth group through O atom has the lowest value when adding 3 OZn molecules reflecting highest reactive structure among them. Table 5 shows that, for the fourth group, IP equal -7.599, -8.761, -10.619, -8.820 and -9.823 eV for Term 1 Na Alg - 3PVA- Mid 1 Na Alg -(1OZn-5OZn) respectively.

3.5 Thermal parameters

Thermal parameters such as enthalpy, entropy, heat capacity, free energy, and heat of formation for the studied structures using PM6 at 298 Kelvin are calculated. The calculated parameters have vital role to describe the physical behavior of system and determine its possible interaction with its surrounding medium in the presence of heat. Enthalpy is defined as the internal energy of system in addition to the product of its pressure and volume. In another words enthalpy express about the total energy of the system. Change in enthalpy is indicator to energy transfer between the system and it's environmental, i.e if change in enthalpy is positive, this means endothermic process. If change in enthalpy is negative this means exothermic process. Then entropy is a measurement to the number of specific ways in which the system may be arranged. Meanwhile, the definition of heat capacity of a specific substance is equal to the amount of energy required to raise its temperature by one degree. Free energy is a measurement to the ability of system to do work. i.e is the energy in system that can be converted to do work. Heat of formation, it can be defined as the change in the enthalpy which during the formation of one mole of a substance from its elements in their natural and standard states, at a given temperature under atmospheric standard conditions.

In the first group ZnO interact with 3PVA- C_{10} 2 Na Alg structure through Zn atom. The value of enthalpy for structures 3PVA - C_{10} 2 Na Alg decorated by different units of ZnO increasing with increase temperature from 200 to 500 K as shown in figure (13-a). The structure 3PVA- C_{10} 2 Na Alg - 5ZnO has enthalpy 20.796 Cal/Mole at temperature 200 K, Meanwhile, enthalpy for 3PVA – C_{10} 2 Na Alg was 13.490 Cal/Mole. The behavior which describes the change of entropy with temperature shown in figure (13-b). This behavior showed that entropy increased with the increase of temperature and also with increasing number of ZnO units. The value of entropy at 200 K was 207.633 for 3PVA – C_{10} 2 Na Alg but, for 3PVA- C_{10} 2 Na Alg - 5ZnO

was 369.893 and 499.233 Cal/K/Mole at 200 and 500 K respectively. Meanwhile, for 3PVA- C_{10} 2 Na Alg - 5ZnO was 169.003 and 287.672Cal/K/Mole at 200 and 500 K respectively. As shown in figure (13-c) the values of heat capacity increased by increasing temperature. The value of heat capacity for 3PVA – C_{10} 2 Na Alg was 111.910 Cal/Mole/K. Addition of ZnO units leads to increase the heat capacity value in most structure. But there is only one structure 3PVA- C_{10} 2 Na Alg - 3ZnO has values of heat capacity lower than the non-decorated structure. Also, figure (13-d) showed that increasing number of ZnO units leads to decrease the value of free energy. But, 3PVA- C_{10} 2 Na Alg - 5ZnO structure has free energy higher than 3PVA- C_{10} 2 Na Alg - 3ZnO and 3PVA- C_{10} 2 Na Alg - 4ZnO structure. Temperature has opposite effect with increasing temperature the value of free energy increased. Free energy for 3PVA – C_{10} 2 Na Alg was the higher value; it means that interaction with ZnO leads to decrease the value of free energy. Meanwhile, for the third thermal parameter which is the heat of formation, the value for 3PVA- C_{10} 2 Na Alg was the higher value - 830.673 Kcal/mol. The behavior of HF with temperature is as shown in figure (13-e). From the figure, it is clear that the temperature does not affect the heat of formation values but, increasing the number of ZnO units leads to decreasing the value of HF for decorated structure. Also, the figure indicated that increasing the number of ZnO units beyond 4, HF starts to increase.

In the second group ZnO interact with 3PVA- C_{10} 2 Na Alg structure through O atom. Figure (14-a) shows the dependence of enthalpy on temperature for the different 3PVA- C_{10} 2 Na Alg structures that decorated with 1, 2, 3, 4 and 5 ZnO units. As shown in the same figure enthalpy increased by increasing temperature and OZn units where 3PVA- C_{10} 2 Na Alg – 5OZn structure has the highest value of enthalpy. Entropy shows linear behavior with increasing temperature as presented in figure (14-b) where entropy increased also. Additionally, the figure indicated that with increasing the number of ZnO units, the value of entropy increased. But, 3PVA- C_{10} 2 Na Alg – 2OZn structure has values of entropy less than 3PVA- C_{10} 2 Na Alg – 1OZn structure. Figure (14-c) shows the behavior of heat capacity with temperature. As shown the values of heat capacity increased by increasing of temperature. Also, noticed that increase the number of ZnO unit leads to increase the heat capacity value of decorated structure. But, only 3PVA- C_{10} 2 Na Alg – 1OZn structure has different behavior where its heat capacity values are the lowest value. The behavior of free energy and heat of formation are the same as shown in figures (14-d and e). With the increase of the value of temperature the values of free energy and heat of formation increased. But, increasing the number of added ZnO units lead to different behavior. Where the values of free energy and heat of formation decreased with increasing temperature. Only 3PVA- C_{10} 2 Na Alg – 5OZn structure has value higher than 3PVA- C_{10} 2 Na Alg – 3OZn structure and 3PVA- C_{10} 2 Na Alg – 4OZn structure, and is near to the value of 3PVA- C_{10} 2 Na Alg – 4OZn structure.

In the third group ZnO interact with Term 1 Na Alg - 3PVA- Mid 1 Na Alg structure through Zn atom. The behavior of enthalpy shown in figure (15-a). The enthalpy values increased with increasing of temperature for all structures. Meanwhile, increase the number of added ZnO unit leads to the increase of enthalpy. But, it's noticed that Term 1 Na Alg - 3PVA- Mid 1 Na Alg - 1ZnOand Term 1 Na Alg - 3PVA- Mid 1 Na Alg - 2ZnO structures have very closed values. Also, the values of Term 1 Na Alg - 3PVA- Mid 1 Na Alg - 3ZnO and Term 1 Na Alg - 3PVA- Mid 1 Na Alg - 4ZnO structures are nearly the same values. As noticed, Term 1 Na Alg - 3PVA- Mid 1 Na Alg - 5ZnO structure has the higher values. Figure (15-b) present behavior of entropy with temperature. Where increase of temperature leads to linear increment of entropy. Also, increasing ZnO number leads to increasing the entropy for doped structure. But, Term 1 Na Alg - 3PVA- Mid 1 Na Alg - 4ZnO structure has values less than Term 1 Na Alg - 3PVA- Mid 1 Na Alg - 3ZnO structure and almost closed to Term 1 Na Alg - 3PVA- Mid 1 Na Alg - 2ZnO structure values. Meanwhile, the heat capacity behavior is presented in figure (15-c) and appeared that increasing temperature leads to increase the heat capacity values. Also, that the heat capacity increased by increasing the number of ZnO units. But, the heat capacity values for Term 1 Na Alg - 3PVA- Mid 1 Na Alg - 1ZnO and Term 1 Na Alg - 3PVA- Mid 1 Na Alg - 2ZnO structures are nearly closed to each other. The figure also indicated that Term 1 Na Alg - 3PVA- Mid 1 Na Alg - 3ZnOand Term 1 Na Alg - 3PVA- Mid 1 Na Alg - 4ZnO structures have the same heat capacity. Figures (15-d and e) presented the behavior of free energy and heat of formation. As depicted in the figure, increasing the temperature the values of both free energy and heat of formation increased. Meanwhile, increasing the number of added ZnO leads to the reduction of the values of both free energy and heat of formation. But, Term 1 Na Alg - 3PVA- Mid 1 Na Alg - 3ZnO structure has different behavior; it has the lower value of free energy and heat of formation by comparison with the other structures.

Finally, for the fourth group, in which ZnO interact with Term 1 Na Alg - 3PVA- Mid 1 Na Alg structure through O atom. The observed behavior of enthalpy is presented in figure (16-a), where the values of enthalpy increased with increasing the temperature. Also, the values of enthalpy increase gradually by increasing the number of added ZnO units from 1 to 5 units. Entropy behavior showed in

figure (16-b) indicated that with temperature increasing, the value of entropy increased. Also, increasing the number of added ZnO units leads to the increase of entropy for decorated structures. But, it's noticed that the values of entropy for Term 1 Na Alg - 3PVA- Mid 1 Na Alg - 4OZn structure has values nearly closed to 3PVA- C_{10} 2 Na Alg - 3OZn structure. The behavior of heat capacity is illustrated in figure (16-c), where increasing the temperature and the number of added ZnO units leads to the enhancement of heat capacity. Figures (16- d and e) present the behavior of free energy and heat of formation where they have the same behavior. As noticed, free energy and heat of formation increased with increasing the temperature. Meanwhile, with increase the number of added ZnO units the value of free energy and HF decreased. But, the values for Term 1 Na Alg - 3PVA- Mid 1 Na Alg - 2OZn structure are higher than Term 1 Na Alg - 3PVA- Mid 1 Na Alg - 1OZn structure.

4. Conclusion

Quantum mechanical calculations of DFT are utilized to study the influence of ZnO on the studied system of PVA/ Na Alg. Based on the obtained results, it is stated that the physical properties of the supposed models of blended PVA and Na Alg are changed due to the decoration with ZnO. The results indicated that the studied physical properties suffer strong changes in both cases of interaction (i.e. interaction proceeds through oxygen or zinc atom). Where, the electronic properties of 3PVA- (C_{10}) 2 Na Alg and Term 1 Na Alg - 3PVA- Mid 1 Na Alg are changed strongly due to decoration. As, for 3PVA- (C_{10}) 2 Na Alg, TDM increased to 89.8929 Debye and HOMO/LUMO energy decreased to 0.2612 eV when it decorated with two units of ZnO. However, for the inverse interaction, TDM decreased to 5.3791 Debye and HOMO/LUMO energy increased to 0.3306 eV. On the other hand, the reverse behaviour took place for the system of Term 1 Na Alg - 3PVA- Mid 1 Na Alg. Where for the decoration through the metal, TDM decreased and HOMO/LUMO energy increased. Meanwhile, for decoration through the oxygen atom, TDM increased and HOMO/LUMO energy decreased. Additionally, MESP results confirmed that the reactivity of 3PVA- (C_{10}) 2 Na Alg and Term 1 Na Alg - 3PVA- Mid 1 Na Alg was affected strongly by decoration with metal oxide. QSAR results also indicated that. All these changes occurred in the electronic properties of the studied structures as a result of the interaction with metal oxide (ZnO) dedicates that ZnO can act as a sensor for PVA/ Na Alg systems. The calculated QSAR descriptors ensure the results obtained from DFT calculations. As well as, the study of thermal parameters confirmed the results of electronic and QSAR parameters. As the results obtained reflecting higher reactive structures, this verifies the impact of modifying the proposed polymer blend with metal oxide nanomaterial regarding their physical and electronic characteristics.

5. References

[1] Sachan K.N., Pushkar S., Jha A., Bhattcharya A.; Sodium alginate: the wonder polymer for controlled drug delivery, Journal of Pharmacy Research, 2, 1191-1199 (2009).

[2] Sun X., Chen J.H., Su Z.B., Huang Y.H., Dong X.F.; Highly effective removal of Cu(II) by a novel 3-aminopropyltriethoxysilane functionalized polyethyleneimine/sodium alginate porous membrane adsorbent, Chemical Engineering Journal, 290, 1-11 (2016).

[3] Wang Q., Ju J., Tan Y., Hao L., Ma Y., Wu Y., Zhang H., Xia Y., Sui K. Controlled Synthesis of Sodium Alginate Electrospun Nanofiber Membranes for Multi-occasion Adsorption and Separation of Methylene Blue, Carbohydrate Polymers, 205, 125-134 (2019).

[4] Bidarra S.J., Barrias C.C., Granja P.L.; Injectable alginate hydrogels for cell delivery in tissue engineering, Acta Biomaterialia, 10, 1646-62 (2014).

[5] Guiping M., Dawei F., Liu Y., Zhu X., Nie J.; Electrospun sodium alginate/poly (ethylene oxide) core–shell nanofibers scaffolds potential for tissue engineering applications, Carbohydrate Polymers, 87, 737-743 (2012).

[6] Han Y., Zeng Q., Li H., Chang J.; The calcium silicate/alginate composite: preparation and evaluation of its behavior as bioactive injectable hydrogels, Acta Biomaterialia, 9, 9107-17 (2013).

[7] Remminghorst U., Rehm B.H.A.; Bacterial alginates: from biosynthesis to applications, Biotechnology Letters, 28, 1701-1712 (2006).

[8] Yang J.S., Xie Y.J., He W.; Research progress on chemical modification of alginate: a review, Carbohydrate Polymers, 84, 33–39 (2011).

[9] Bi S., Hou L., Lu Y.; Multifunctional sodium alginate fabric based on reduced graphene oxide and plypyrrole for wearable closed-loop point-of-care application, Chemical Engineering Journal, 406, 126778 (2021).

[10] Swaminathan A., Ravi R., Sasikumar M., Dasaiah M., Hirankumar G., Ayyasamy S.; Preparation and characterization of PVA/PAM/NH4SCN polymer film by

ultrasound-assisted solution casting method for application in electric double layer capacitor, Ionics, 26, 4113–4128 (2020).

[11] Demerlis C.C., Schoneker D.R.; Review of the oral toxicity of polyvinyl alcohol (PVA), Food and Chemical Toxicology, 41, 319–326 (2003).

[12] Maria T.M., Carvalho R.A., Sobral P.J., Habitantea A.M., Solorza-Feriab J.; The effect of the degree of hydrolysis of the PVA and the plasticizer concentration on the color, opacity, and thermal and mechanical properties of films based on PVA and gelatin blends, Journal of Food Engineering , 87, 191–199 (2008).

[13] Qiu K., Netravali A.N.; Fabrication and characterization of biodegradable composites based on microfibrillated cellulose and polyvinyl alcohol, Composites Science and Technology, 72, 1588– 1594 (2012).

[14] Qiu K., Netravali A.N.; A Composting Study of Membrane Like Polyvinyl Alcohol Based Resins and Nanocomposites, Journal of Polymers and the Environment , 21, 658–674 (2013).

[15] Qiu K., Netravali A.N.; Halloysite nanotube reinforced biodegradablenanocomposites using noncrosslinked and malonic acid crosslinked polyvinyl alcohol, Polymer composite , 34, 799–809 (2013).

[16] Ibrahim M., Osman O.; Spectroscopic Analyses of Cellulose: Fourier Transform Infrared and Molecular Modelling Study, Journal of Computational and Theoretical Nanoscience, 6, 1054–1058 (2009).

[17] Ibrahim M., Osman O., Mahmoud A.A.; Spectroscopic Analyses of Cellulose and Chitosan: FTIR and Modeling Approach, Journal of Computational and Theoretical Nanoscience, 8, 117-123 (2011).

[18] Quynh N.P.L.P., , Thi T.U.D., Tran C.V., Vu H.N., , Ta H.K.T. , Tran C.V., Phan T.B., Pham N.K.; Improving memory performance of PVA:ZnO nanocomposite: The experimental and theoretical approaches, Applied Surface Science, 537, 148000 (2021).

[19] Khatir N.M., Abdul-Malek Z., Zak A.K., Akbar A., Sabbagh F.; Sol–gel grown Fe-doped ZnO nanogranule: antibacterial and structural behaviors, Journal of Sol-Gel Science and Technology, 78, 91-98 (2016).

[20] Norouzi M.A., Montazer M., Harifi T., Karimi P.; Flower buds like PVA/ZnO composite nanofibers assembly: Antibacterial, in vivo wound healing, cytotoxicity and histological studies, Polymer Testing 93, 106914 (2021).

[21] Raghupathi K.R., Koodali R.T., Manna A.C.; Size-dependent bacterial growth inhibition and mechanism of antibacterial activity of zinc oxide nanogranule, Langmuir, 27, 4020-4028 (2011).

[22] Ozkan E., Ozkan F.T., Allan E., Parkin I.P.; The use of zinc oxide nanogranule to enhance the antibacterial properties of light-activated polydimethylsiloxane containing crystal violet, RSC Advances, 5, 8806 (2015).

[23] Kumar A., Mahto V., Choubey a.K.; Synthesis and characterization of cross-linked hydrogels using polyvinyl alcohol and polyvinyl pyrrolidone and their blend for water shut-off treatments, Journal of Molecular Liquids, 301, 112472 (2020).

[24] Hezma A. M., Rajeh A., Mannaa M. A.; An insight into the effect of zinc oxide nanoparticles on the structural, thermal, mechanical properties and antimicrobial activity of Cs/PVA composite, Colloids and Surfaces A, 581, 123821 (2019).

[25] Kumar S., Krishnakumar B., Sobral A. J.F.N., Koh J.; io-based (chitosan/PVA/ZnO) nanocomposites film: Thermally stable and photoluminescence material for removal of organic dye, Carbohydrate Polymers, 205, 559-564 (2019).

[26] Darbasizadeh B., Fatahi Y., Feyzi-barnaji B., Arabi M., Motasadizadeh H., Farhadnejad H., Moraffah F., Rabiee N.; Crosslinked-polyvinyl alcohol-carboxymethyl cellulose/ZnO nanocomposite fibrous mats containing erythromycin(PVA-CMC/ZnO-EM): Fabrication, characterization and in-vitro release and anti-bacterial properties, International Journal of Biological Macromolecules, 141, 1137-1146 (2019).

[27] Patil P. P., Bohara R. A., Meshram J. V., Nanaware S. G., Pawar S. H.; Hybrid chitosan-ZnO nanoparticles coated with a sonochemical technique on silk fibroin-PVA composite film: A synergistic antibacterial activity, International Journal of Biological Macromolecules 122, 1305-1312 (2019).

[28] Dodero A., Alloisio M., Vicini S., Castellano M.; Preparation of composite alginate-based electrospun membranes loaded with ZnO nanoparticles, Carbohydrate Polymers, 227, 115371 (2020).

[29] Raguvaran R.,Manuja B.K., Chopra M., Thakur R., Anand T., Kalia A., Manuja A.; Sodium alginate and gum acacia hydrogels of ZnO nanoparticles show wound healing effect on fibroblast cells, International Journal of Biological Macromolecules, 96, 185-191 (2017).

[30] Varaprasad K., Raghavendra G.M., Jayaramudu T., Seo J.; Nano zinc oxide–sodium alginate

antibacterial cellulose fibres, Carbohydrate Polymers, 135, 349-355 (2016).

[31] Alavi M., Nokhodchi A.; An overview on antimicrobial and wound healing properties of ZnO nanobiofilms, hydrogels, and bionanocomposites based on cellulose, chitosan, and alginate polymers, Carbohydrate Polymers, 227, 115349 (2020).

[32] Ibrahim M.; Molecular Modeling and FTIR Study for K, Na, Ca and Mg Coordination with Organic Acid, Journal of Computational and Theoretical Nanoscience, 6, 682–685 (2009).

[33] El-Sayed E. M., Omar A., Ibrahim M., Abdel-Fattah W. I.; On the Structural analysis and Electronic Properties of Chitosan /Hydroxyapatite Interaction, Journal of Computational and Theoretical Nanoscience, 6, 1663-1669 (2009).

[34] Youness R. A., Taha M. A., Elhaes H., Ibrahim M.; Molecular Modeling, FTIR Spectral Characterization and Mechanical Properties of Carbonated-Hydroxyapatite Prepared by Mechanochemical Synthesis, Materials Chemistry and Physics, 190, 209-218 (2017).

[35] Grenni P., Caracciolo A. B., Mariani L., Cardoni M., Riccucci C., Elhaes H., Ibrahim M. A.; Effectiveness of a new green technology for metal removal from contaminated water, Microchemical Journal, 147, 1010-1020 (2019).

[36] Han M.; Exchange of macromolecules and colloids in a dense medium: A molecular simulation method, Journal of Computational Physics, 395, 263-274 (2019).

[37] Ajayi T. J., Shapi M.; Solvent-free mechanochemical synthesis, hirshfeld surface analysis, crystal structure, spectroscopic characterization and NBO analysis of Bis(ammonium) Bis((4-methoxyphenyl) phosphonodithioato)-nickel (II) dihydrate with DFT studies, Journal of Molecular Structure, 1202, 127254 (2020).

[38] Fahmy A., Khafagy R. M., Elhaes H., Ibrahim M. A.; Molecular Properties of Polyvinyl Alcohol/Sodium Alginate Composite, Biointerface Research in Applied Chemistry 10, 4734-4739 (2020).

[39] Frisch M.J., Trucks G.W., Schlegel H.B., Scuseri G. E ,Robb M.A., Cheeseman J.R., Scalmani G., Barone V., Mennucci ,Petersson B. G. A., Nakatsuji H., Caricato M., Li X., HratchianP.H ,. Izmaylov A.F., Bloino J., Zheng G., Sonnenberg J.L., Hada M.,Ehara M., Toyota K., Fukuda R., Hasegawa J., Ishida M., Nakajima,T . Honda Y., Kitao O., Nakai H., Vreven T., Montgomery J.A., Jr ,.Peralta J.E., Ogliaro F., Bearpark M., Heyd J.J., Brothers,E .Kudin K.N., Staroverov V.N., Keith T., Kobayashi R., Normand,J , . Raghavachari K.,, Rendell A.,, Burant J.C., Iyengar S.S., Tomasi J., ,Cossi M., Rega N., Millam J.M., Klene M., Knox J.E., Cross J.B., , Bakken V., Adamo C., Jaramillo J., Gomperts R., StratmannR.E., , Yazyev O., Austin A.J., Cammi R., Pomelli C., Ochterski J.W., , Martin R.L., Morokuma K., Zakrzewski V.G., Voth G.A., Salvador P., Dannenberg J.J., Dapprich S., DanielsA.D., ,Farkas, O., Foresman J.B., Ortiz J.V., Cioslowski J., ,Fox D.J., Gaussian, Inc., Gaussian 09, Revision C.01.Wallingford CT (2010).

[40] Becke A.D.; Density functional thermochemistry. III. The role of exact exchange, Journal of Chemical Physics, 98, 5648-5652 (1993).

[41] Lee C., Yang W., Parr R.G.; Development of the Colle-Salvetti correlation-energy formula into a functional of the electron density, Physical Review B, 37, 785 (1988).

[42] Miehlich B., Savin A., Stoll H., Preuss H.; Results obtained with the correlation energy density functionals of becke and Lee, Yang and Parr., Chemical Physics Letters . 157, 200 (1989).